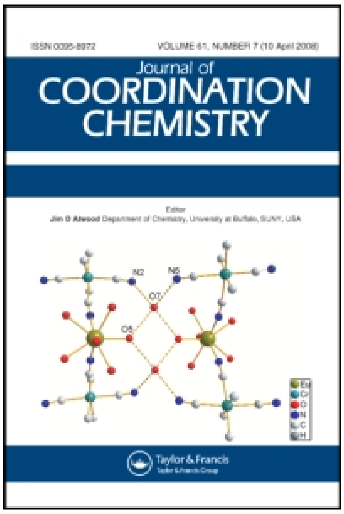

Journal of Coordination Chemistry
Publication details, including instructions for authors and subscription information:
http://www.informaworld.com/smpp/title~content=t713455674

XAFS spectroscopic study of $Tc_2(O_2CCH_3)_4X_2$ (X = Cl, Br)

Frederic Poineau[a]; Alfred P. Sattelberger[ab]; Kenneth R. Czerwinski[a]
[a] Harry Reid Center for Environmental Studies, University of Nevada Las Vegas, Las Vegas, NV 89154 [b] Physical Sciences Directorate, Argonne National Laboratory, Argonne, IL 60439

To cite this Article Poineau, Frederic , Sattelberger, Alfred P. and Czerwinski, Kenneth R.(2008) 'XAFS spectroscopic study of $Tc_2(O_2CCH_3)_4X_2$ (X = Cl, Br)', Journal of Coordination Chemistry, 61: 15, 2356 — 2370
To link to this Article: DOI: 10.1080/00958970801927092
URL: http://dx.doi.org/10.1080/00958970801927092

Journal of Coordination Chemistry
Vol. 61, No. 15, 10 August 2008, 2356–2370

Taylor & Francis
Taylor & Francis Group

XAFS spectroscopic study of $Tc_2(O_2CCH_3)_4X_2$ ($X = Cl$, Br)

FREDERIC POINEAU*†, ALFRED P. SATTELBERGER†‡ and KENNETH R. CZERWINSKI†

†Harry Reid Center for Environmental Studies, University of
Nevada Las Vegas, Las Vegas, NV 89154
‡Physical Sciences Directorate, Argonne National Laboratory,
9700 Cass Avenue, Argonne, IL 60439

(*Received 21 September 2007; in final form 2 January 2008*)

Technetium dimers $Tc_2(O_2CCH_3)_4X_2$ ($X = Cl$, Br) were synthesized and studied by X-ray Absorption Fine Structure spectroscopy (XAFS). EXAFS analysis gave for $Tc_2(O_2CCH_3)_4Cl_2$: d Tc-Tc = 2.18(1) Å, d Tc–Cl = 2.43(1) Å and for $Tc_2(O_2CCH_3)_4Br_2$: d Tc–Tc = 2.19(1) Å, d Tc-Br = 2.63(1) Å. The Tc Tc separations are in agreement with Raman studies while the Tc–X distances are somewhat larger. Comparison with other Tc(III) quadruply bonded dimers indicates that the carboxylate compounds exhibit larger Tc–Tc separations. The effect of the terminal ligand (nature and position) on the Tc–Tc separation is discussed.

Keywords: Technetium; quadruply bonded dimers; carboxylate; EXAFS

1. Introduction

Technetium occupies a central position in the Periodic Table. Thirty four isotopes of the element are known with mass numbers ranging from 85 to 118 and all are radioactive. The most readily available isotope is ^{99}Tc ($t_{1/2} = 2.1 \times 10^5$ y) which is isolated in large quantities from spent nuclear fuel where it constitutes approximately 6% of the fission yield (via ^{99}Mo). Ammonium pertechnetate, $(NH_4)TcO_4$, is the most common, readily obtainable salt. All other starting materials trace their origins to $(NH_4)TcO_4$. The radioactive nature of technetium and the associated costs of radiological laboratories explain why its chemistry has not developed to the extent of its Mn and Re congeners.

Technetium dimers containing a quadruple metal-metal bond are a relatively new addition to the family of Tc compounds and are interesting from the point of view of structure and bonding. As reported in a recent monograph [1], only five technetium quadruply bonded dimers have been characterized structurally.

Our recent research on technetium chemistry has focused on the expansion of the family of quadruply bonded Tc(III) dimers. Recently [2], reliable syntheses of $(n\text{–}Bu_4N)_2Tc_2X_8$ (X=Cl, Br) were developed in our laboratory which led to XAFS and UV-Vis studies aimed at elucidating the structures and spectroscopic properties of

---

*Corresponding author. Email: freder29@unlv.nevada.edu

Journal of Coordination Chemistry
ISSN 0095-8972 print/ISSN 1029-0389 online © 2008 Taylor & Francis
DOI: 10.1080/00958970801927092

these compounds. Carboxylate derivatives of the type $Tc_2(O_2CCR)_4X_2$ (R = Me, t-Bu; X = Cl, Br) can be prepared from these starting materials [3–6] but only one of these (R = t-Bu) has been characterized by X-ray crystallography [6]. The acetate derivatives (R = Me) have been studied by Raman spectroscopy, IR and x-ray powder diffraction. The acetate compounds, obtained as microcrystalline powders, are insoluble in most solvents which precludes re-crystallization into single crystals suitable for XRD.

As has been shown for many technetium compounds [7–9], EXAFS spectroscopy is an efficient technique in the determination of structural parameters. We report here EXAFS spectra of $Tc_2(O_2CCH_3)_4X_2$ (X = Cl, Br), the structural parameters derived therefrom, and a comparison with the other known technetium quadruply bonded compounds.

2. Experimental

2.1. *Synthesis of compounds*

Caution. Techetium-99 is a weak beta emitter ($E_{\max} = 292$ keV). All manipulations were performed in a laboratory designed for work with radioactive materials using efficient HEPA-filtered fume hoods, Schlenk and glove box techniques, and following locally approved nuclear chemistry handling and monitoring procedures. Lab coats, disposable gloves and protective eyewear were worn at all times.

$(NH_4)TcO_4$ was purchased from Oak Ridge National Laboratory. The compound contains a black impurity; prior to use, it was purified and converted to $(n\text{–}Bu_4N)TcO_4$. The solvents and reagents, i.e., THF, acetone, ether, $(n\text{–}Bu_4N)BH_4$, $(n\text{–}Bu_4N)HSO_4$, CH_2Cl_2, hexane, 12 M HCl, acetic acid and acetic anhydride were purchased from Sigma-Aldrich and used as received. HBr gas was purchased as a lecture bottle from Matheson and used as received.

Preparation of $(n\text{–}Bu_4N)TcO_4$. 250 mg of $(NH_4)TcO_4$ (1.381 mmol) was dissolved in 5 mL of deionized (DI) water and the solution transferred to a 15 mL glass centrifuge tube. Then 600 mg (1.760 mmol) of $(n\text{–}Bu_4N)HSO_4$ dissolved in 5 mL of DI water were added dropwise, and the voluminous white $(n\text{–}Bu_4N)TcO_4$ precipitated. The suspension was centrifuged, the supernatant removed, and the solid washed with 10 mL of ice cold water. After drying over Drierite for 24 h in a desiccator, 532 mg (1.310 mmol) was recovered; yield, 94.8%.

Preparation of $(n\text{–}Bu_4N)TcOCl_4$. Ten mL of 12 M HCl was added to the 532 mg of $(n\text{–}Bu_4N)TcO_4$, a small magnetic stir bar was added, and the suspension was stirred for 30 minutes at room temperature. Voluminous green $(n\text{–}Bu_4N)TcOCl_4$ precipitated. The compound was centrifuged, the supernatant was removed and discarded. The solid was treated a second time with 10 mL of fresh, cold 12 M HCl. After centrifugation, the supernate was decanted and the green $(n\text{–}Bu_4N)TcOCl_4$ was dried in a vacuum dessicator overnight. The solid was recrystallized from a mixture of (minimal) acetone/ether and 584 mg were obtained (1.168 mmol); yield, 89.1%.

Preparation of $(n\text{–}Bu_4N)_2Tc_2Cl_8$. Tetrabutylammonium octachloro- and octabromo ditechnetate were synthesized by a modification [2] of the method of Preetz and coworkers [10]. The reaction was performed in a 250 mL round bottom flask equipped with a 3-hole rubber stopper. 543 mg (1.086 mmol) of $(n\text{–}Bu_4N)TcOCl_4$ was dissolved in

10 mL of THF and the solution was purged for 10 minutes with Ar. A solution of (n–Bu_4N)BH_4 (563 mg, 2.187 mmol) in 20 mL of THF was added dropwise under Ar. Ten minutes after the addition, 50 mL of air-free ether was added slowly to the solution. The argon bubbling was stopped and the flask closed with a rubber septum. A brown oil was observed at the bottom of the flask. After 30 minutes, the ether was removed, the flask was placed in a vacuum desiccator and the oil was pumped to dryness (~14–16 h). The resulting brown powder was dissolved in 8 mL of acetone and 380 µL of 12 M HCl was slowly added dropwise while stirring. After 5 minutes, 12 mL of pre-cooled (5°C) ether was slowly added to the stirred solution and a green precipitate appeared; the flask was stored overnight at −25°C (freezer). The brown supernatant was removed, and the green/brown solid was washed with a minimal volume of acetone. The resulting green solid was re-crystallized two times from minimal CH_2Cl_2/hexane. 342 mg (0.359 mmol) (n–Bu_4N)$_2Tc_2Cl_8$ was obtained (yield, 66.1%). The compound was characterised by UV-Vis spectroscopy.

Preparation of (n–Bu_4N)$_2Tc_2Br_8$. 166 mg (0.174 mmol) sample of (n–Bu_4N)$_2Tc_2Cl_8$ was dissolved in 15 mL of dichloromethane in a 100 mL round bottom flask and purged with argon. The solution was warmed to 30°C in an oil bath. Simultaneously with the Ar stream, a stream of HBr(g) was passed through the solution which turns from green to red. After 15 minutes, the flow of HBr was stopped and the solution evaporated to dryness with the argon stream. The red solid was dissolved in minimal boiling dichloromethane and then cooled 6 h at −25°C. 159 mg (0.119 mmol) of microcrystalline (n–Bu_4N)$_2Tc_2Br_8$ was obtained (68.5%) after removal of the supernate and drying under vacuum. The compound was characterised by UV-Vis spectroscopy.

Preparation of $Tc_2(O_2CCH_3)_4Cl_2$. 150 mg (0.157 mmol) of (n–Bu_4N)$_2Tc_2Cl_8$ was dissolved/suspended in a mixture of 8 mL acetic acid and 2 mL^{-1} acetic anhydride in a 50 mL Schlenk flask. The suspension was heated in an oil bath (130°C) and boiled for 20 minutes under argon with stirring. After 10 minutes, the solution turned from green to orange and a red/orange precipitate was observed. The suspension was cooled to room temperature under argon, transferred to a 15 mL centrifuge tube, and centrifuged for several minutes. The supernatant was removed with a disposable glass pipette and the compound washed with acetone (2 × 5 mL) and ether (2 × 5 mL). A cherry red compound (32.3 mg, 0.063 mmol) was obtained. Yield = 40.5%.

Preparation of $Tc_2(O_2CCH_3)_4Br_2$. 44.1 mg (0.033 mmol) of (n–Bu_4N)$_2Tc_2Br_8$ was suspended in a mixture of 10 mL acetic acid and 2 mL^{-1} acetic anhydride in a 50 mL Schlenk flask. The suspension was boiled for 3 minutes under Ar with stirring, whereupon an orange precipitate was observed. As for the chloro derivative, the solution was cooled to room temperature under argon. The suspension was centrifuged, the supernatant removed and the precipitate washed with acetone (2 × 5 mL) and ether (2 × 5 mL). An orange compound (15.5 mg, 0.026 mmol) was obtained. Yield = 78.6%.

2.2. *XAFS measurements*

XAFS measurements were done at the Advanced Photon Source (APS) at the BESSRC-CAT 12 BM station at Argonne National Laboratory. Technetium compounds were diluted (~1% Tc in mass) in boron nitride, ground in a mortar, and a fraction (~20 mg) was packed in a polycarbonate cavity, covered with kapton tape (0.25 µm) and placed in an aluminum sample holder of local design. XAFS spectra were recorded at the Tc-K edge (21,044 eV) in fluorescence mode at room temperature using a 13 elements germanium detector. The Tc concentration permits one to obtain fluorescence spectra without significant self absorption. A double crystal of Si [1 1 1] was used as a monochromator. The energy was calibrated using a molybdenum foil (Mo-K edge = 20,000 eV). For each sample, four spectra were recorded in the k range [0–14] Å^{-1} and averaged. Background contribution was removed using AutoBk [11] software and data analysis was performed using Winxas [12]. For the fitting procedure, amplitude and phase shift function were calculated by Feff8.2 [13]. Input files were generated by Atoms [14] using crystallographic structures of the tetrapivalate dihalide rhenium(III) complexes [15]. Adjustments of the k^2-weighted EXAFS spectra were performed under the constraints $S_0^2 = 0.9$ (S_0^2 refers to the amplitude reduction factor; the value 0.9 is currently used for fitting of Tc compounds [9, 16]). A single value of energy shift (ΔE_0) was used for all scattering. The uncertainty determined by EXAFS on the coordination number is ±20% and ±0.01 Å on the atomic distance. For the spectral simulation studies, the scattering and amplitude function generated by Feff8.2 were extracted, k^2-weighted and Fourier transformed between $k = [3, 14]$ Å^{-1} using Artemis software [17].

3. Results

3.1. *Spectral simulation*

In $Tc_2(O_2CCMe_3)_4X_2$ and $Tc_2(O_2CCH_3)_4X_2$ (X=Cl, Br), the technetium atoms exhibit similar coordination over four atoms shells. Simulated EXAFS spectra of the pivalate dimers, $Tc_2(O_2CCMe_3)_4X_2$, permit one to predict the EXAFS spectra of the acetate dimers, $Tc_2(O_2CCH_3)_4X_2$.

As previously mentioned, X-ray structures of $Tc_2(O_2CCH_3)_4X_2$ (X=Cl, Br) were not available. The X-ray structures of $Re_2(O_2CCMe_3)_4X_2$ (X=Cl, Br) are known and the atomic coordinates were used to simulate EXAFS spectra. A simulation of the Fourier transform of the k^2-EXAFS spectra of $Tc_2(O_2CCMe_3)_4X_2$ (X=Cl, Br) was performed using the atomic coordinates of the Re congeners [15].

The Fourier transform can be explained using four single and three multi-scatterings. The amplitude and path of these major scatterings are presented in table 1; their

Table 1. Main scattering calculated in $Tc_2(O_2CCMe_3)_4X_2$ (X=Cl, Br).

Scattering	Amplitude (%)	Degeneracy	Path
A	33.3, (33.49)	1	$\mathrm{Tc_1 \leftrightarrows Tc_2}$
B	21.15, (18.77)	1	$\mathrm{Tc_1 \leftrightarrows X_1}$
C	100, (100)	4	$\mathrm{Tc_1 \leftrightarrows O_1}$
D	32.44, (32.90)	4	$\mathrm{Tc_1 \leftrightarrows C_1}$
E	34.97, (35.33)	4	$\mathrm{Tc_1 \leftrightarrows O_2}$
F	21.74, (22.52)	8	$\mathrm{Tc_1 {}^{\leftarrow} \underset{\rightarrow}{O_1} {}^{\leftarrow} C_1}$
G	25.73, (25.53)	4	$\mathrm{O_{1b} \leftrightarrows Tc_1 \leftrightarrows O_{1a}}$
H	27.55, (25.73)	1	$\mathrm{Tc_1 \leftrightarrows Tc_2 \leftrightarrows X_2}$

For amplitude (%), values in parenthesis refer to $Tc_2(O_2CCMe_3)_4Br_2$.

contribution to the total Fourier transform are shown in figure 1 for X = Cl and figure 2 for X = Br. These scattering patterns involve the technetium, halogen, carbon and oxygen atoms situated in the first, second and third coordination shell. In order to visualize the atoms involved in the scattering path, a ball and stick representation of $Tc_2(O_2CCH_3)_4X_2$ (X = Cl, Br) is shown in figure 3.

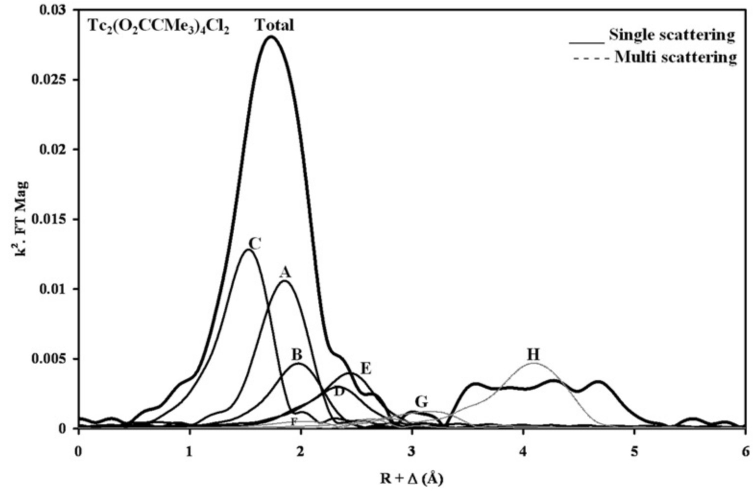

Figure 1. FEFF8.2 simulation of the Fourier transform of the k^2-EXAFS spectra of $Tc_2(O_2CCMe_3)_4Cl_2$. The total FT is shown including: the main single scattering A $(\mathrm{Tc_1} \leftrightarrows \mathrm{Tc_2})$, B $(\mathrm{Tc_1} \leftrightarrows \mathrm{Cl_1})$, C $(\mathrm{Tc_1} \leftrightarrows \mathrm{O_1})$, D $(\mathrm{Tc_1} \leftrightarrows \mathrm{C_1})$, E $(\mathrm{Tc_1} \leftrightarrows \mathrm{O_2})$ and the main multi scattering F $(\mathrm{Tc_1} \leftrightarrows \mathrm{O_1} \leftarrow \mathrm{C_1})$, G $(\mathrm{O_{1b}} \leftrightarrows \mathrm{Tc_1} \leftrightarrows \mathrm{O_{1a}})$ and H $(\mathrm{Tc_1} \leftrightarrows \mathrm{Tc_2} \leftrightarrows \mathrm{Cl_2})$. Simulation between $k = [3, 14]$ Å^{-1}.

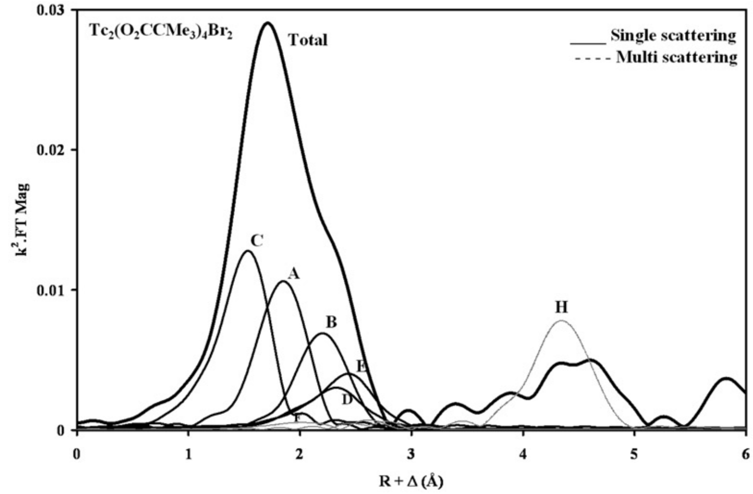

Figure 2. FEFF8.2 simulation of the Fourier transform of the k^2-EXAFS spectra of $Tc_2(O_2CCMe_3)_4Br_2$. The total FT is shown including: the main single scattering A $(\mathrm{Tc_1} \leftrightarrows \mathrm{Tc_2})$, B $(\mathrm{Tc_1} \leftrightarrows \mathrm{Br_1})$, C $(\mathrm{Tc_1} \leftrightarrows \mathrm{O_1})$, D $(\mathrm{Tc_1} \leftrightarrows \mathrm{C_1})$, E $(\mathrm{Tc_1} \leftrightarrows \mathrm{O_2})$ and the main multi scattering F $(\mathrm{Tc_1} \leftrightarrows \mathrm{O_1} \leftarrow \mathrm{C_1})$, G $(\mathrm{O_{1b}} \leftrightarrows \mathrm{Tc_1} \leftrightarrows \mathrm{O_{1a}})$ and H $(\mathrm{Tc_1} \leftrightarrows \mathrm{Tc_2} \leftrightarrows \mathrm{Br_2})$. Simulation between $k = [3, 14]$ Å^{-1}.

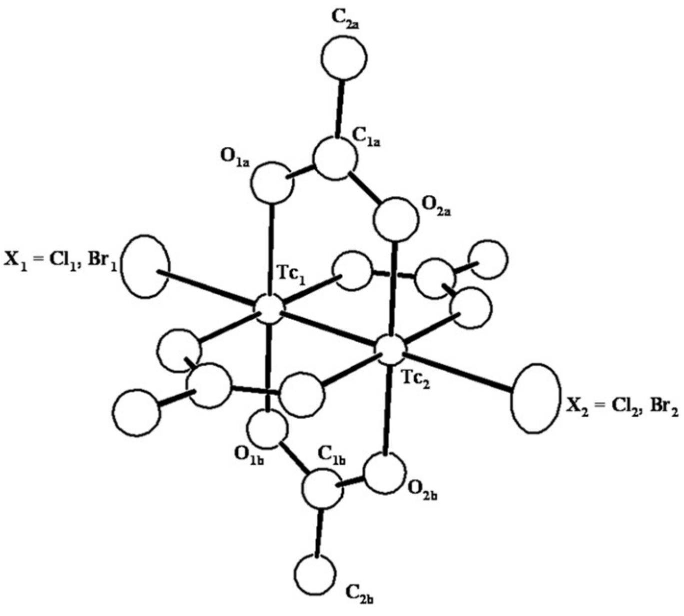

Figure 3. Ball and stick representation of $\mathrm{Tc_2(O_2CCH_3)_4X_2}$ (X = Cl, Br).

For $\mathrm{Tc_2(O_2CCMe_3)_4Cl_2}$, three scattering wave functions ($\mathrm{Tc_1} \leftrightarrows \mathrm{Tc_2}$, $\mathrm{Tc_1} \leftrightarrows \mathrm{O_1}$ and $\mathrm{Tc_1} \leftrightarrows \mathrm{Cl_1}$) overlap in the region $\mathrm{R} + \Delta\mathrm{R} = [1, 2.20]$ Å while for $\mathrm{Tc_2(O_2CCMe_3)_4Br_2}$ five scattering ($\mathrm{Tc_1} \leftrightarrows \mathrm{Tc_2}$, $\mathrm{Tc_1} \leftrightarrows \mathrm{O_1}$, $\mathrm{Tc_1} \leftrightarrows \mathrm{Br_1}$, $\mathrm{Tc_1} \leftrightarrows \mathrm{O_2}$, $\mathrm{Tc_1} \leftrightarrows \mathrm{C_1}$) overlap in the region $\mathrm{R} + \Delta\mathrm{R} = [1, 2.50]$ Å. These regions will be considered for the adjustment procedure. The difference in overlap is due to the shift of the $\mathrm{Tc_1} \leftrightarrows \mathrm{X_1}$ scattering wave functions from 2.40 Å for X = Cl to 2.60 Å for X = Br. The $\mathrm{Tc_1} \leftrightarrows \mathrm{Br_1}$ scattering has strong overlap with the $\mathrm{Tc_1} \leftrightarrows \mathrm{Tc_2}$, $\mathrm{Tc_1} \leftrightarrows \mathrm{O_2}$ and $\mathrm{Tc_1} \leftrightarrows \mathrm{C_1}$ scatterings, while the $\mathrm{Tc_1} \leftrightarrows \mathrm{Cl_1}$ scattering overlaps mainly with the $\mathrm{Tc_1} \leftrightarrows \mathrm{Tc_2}$ scattering.

For both compounds, the multi scatterings with significance amplitude (F, G and H) are those exhibiting a scattering angle of 180°. For this condition, the "focusing effect" is enhanced [18].

3.2. *Adjustment of the EXAFS spectra*

The EXAFS spectra of $\mathrm{Tc_2(O_2CCH_3)_4X_2}$ (X = Cl, Br) were k^2-weighted and a Fourier transformation done in the k-range [4.2, 13.7] Å^{-1}. The adjustments of the experimental EXAFS spectra were performed using the calculated scattering wave functions determined for the Tc(III) pivalate complexes. The procedure was performed in two steps: (a) adjustment between $R + \Delta R = [1, 2.20]$ Å for X = Cl and $R + \Delta R = [1, 2.50]$ Å for X = Br; (b) adjustment of the total spectra using the parameters previously determined in (a).

3.2.1. Analysis of $\mathrm{Tc_2(O_2CCH_3)_4Cl_2}$

a. Adjustment between $R + \Delta R = [1, 2.20]$ Å. A window filter was done on the FT between $R + \Delta R = [1, 2.20]$ Å. The Fourier transform was back transformed and the

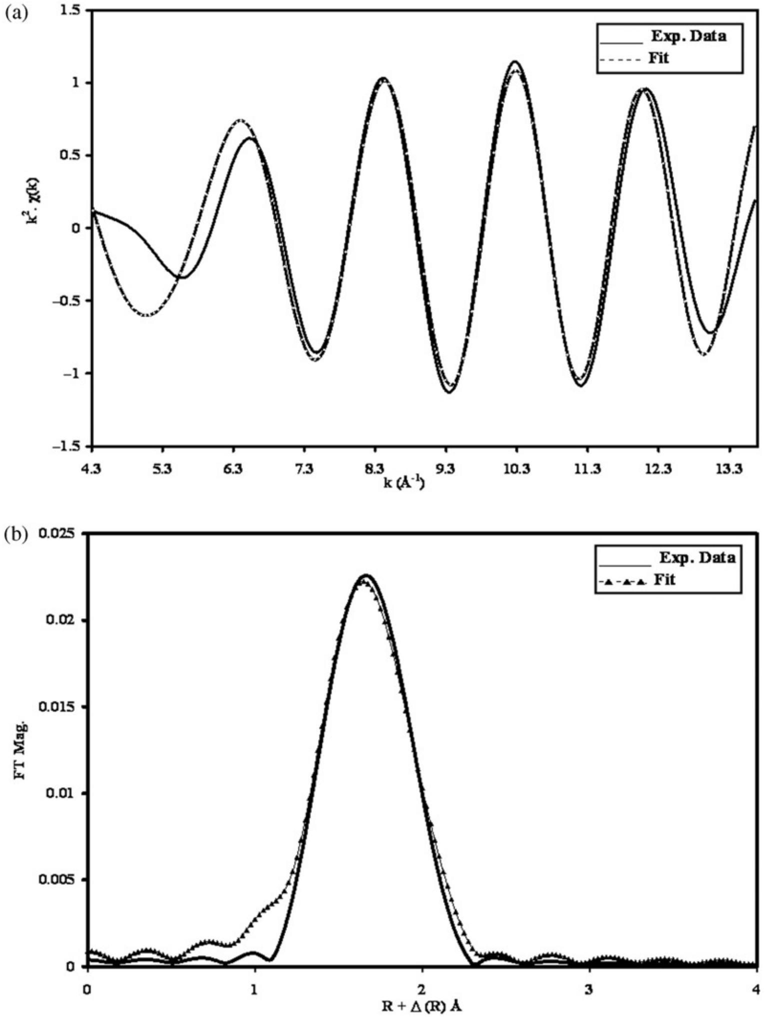

Figure 4. Adjustment of filtered Fourier transform (b) and back transformed k^2-EXAFS (A) spectra of $\mathrm{Tc_2(O_2CCH_3)_4Cl_2}$. Fourier Filtering between $R + \Delta R = [1, 2.20]$ Å; adjustment between $k = [4.2,\ 13.7]$ $\mathrm{\AA^{-1}}$.

corresponding EXAFS spectra fitted in the k-range [4.2, 13.7] $\mathrm{\AA^{-1}}$ using the scattering $\mathrm{Tc_1} \leftrightarrows \mathrm{Tc_2}$, $\mathrm{Tc_1} \leftrightarrows \mathrm{O_1}$, $\mathrm{Tc_1} \leftrightarrows \mathrm{Cl_1}$ determined in **3.1**. The adjustment was conducted with the following procedure:

- In accordance with the stoichiometry $\mathrm{Tc_2(O_2CCH_3)_4Cl_2}$, the number of atoms in the first shell were fixed to four for $\mathrm{O_1}$, one for $\mathrm{Tc_2}$ and one for $\mathrm{Cl_1}$.
- The distances $\mathrm{Tc_1{-}Tc_2}$, $\mathrm{Tc_1{-}O_1}$ and $\mathrm{Tc_1{-}Cl_1}$, and all the σ^2 were allowed to vary.

The fitted k^2-EXAFS spectra and the Fourier transform obtained are presented in figure 4. The results of the adjustments indicate that the first coordination shell around $\mathrm{Tc_1}$, is constituted by one Tc atom at 2.18(1) Å, one Cl atom at 2.43(1) Å and four O atoms at 2.03(1) Å.

b. Adjustment of the total EXAFS spectra. The total EXAFS spectrum was fitted in k-range $[4.2, 13.7]\,\text{Å}^{-1}$ using all major scattering (table 1). Attempts to fit the total EXAFS spectrum by allowing all the parameters to vary simultaneously resulted in an error in the fitting algorithm. The adjustment was conducted according the following procedure:

- In accordance with the stoichiometry $Tc_2(O_2CCH_3)_4Cl_2$, the number of Tc_2, Cl_1 and O_1 atoms in the first coordination shell was fixed (as in **3.2.1.a.**) and the number of the C_1 atoms in the second shell and O_2 atoms in the third shell were fixed to four.
- The distances Tc_1–Cl_1, Tc_1–Tc_2 and the corresponding σ^2 were fixed to those determined in **3.2.1.a.**
- The degeneracy of the multi scattering F, G, and H were fixed to the value determined in **3.1**.
- The distance d Tc_1–O_1 was correlated to the scattering path G: $d\ O_{1b} \leftrightarrows Tc_1 \leftrightarrows O_{1a} = 2\text{x}d\ Tc_1 \leftrightarrows O_1$.
- The distances Tc_1–O_2 and Tc_1–C_1, the scattering length F and H and all the σ^2 were allowed to vary. The fitted Fourier transform and k^2-EXAFS spectra are shown in figure 5. The structural parameters are presented in table 2.

For $Tc_2(O_2CCH_3)_4Cl_2$, the first coordination shell around the absorbing atom has one Tc atom at 2.18(1) Å, one Cl atom at 2.43(1) Å and four O atoms at 2.03(1) Å. The second coordination shell is constituted by four C atoms at 2.86(1) Å and the third coordination shell by four O_2 atoms at 2.97(1) Å.

3.2.2. Analysis of $Tc_2(O_2CCH_3)_4Br_2$

a. Adjustment between $R + \Delta R = [1, 2.50]$ *Å.* A window filter was done on the FT between $R + \Delta R = [1, 2.50]$ Å. The Fourier transform was back transformed and the corresponding EXAFS spectra fitted in the k-range $[4.2, 13.7]$ Å^{-1}. The adjusting procedure was conducted using the five scattering wave functions previously determined: $Tc_1 \leftrightarrows Tc_2$, $Tc_1 \leftrightarrows O_1$, $Tc_1 \leftrightarrows Br_1$, $Tc_1 \leftrightarrows C_1$ and $Tc_1 \leftrightarrows O_2$. The fitting was performed in three iterations.

- The number of atoms was fixed to 1 for Tc_2, 4 for O_1 and 1 for Br_1, the distances $Tc_1\,Tc_2$, $Tc_1\,Br_1$ and Tc_1–O_1 and all the σ^2 were allowed to vary. Since the scattering wave functions $Tc_1 \leftrightarrows Br_1$, $Tc_1 \leftrightarrows C_1$ and $Tc_1 \leftrightarrows O_2$ overlap strongly in the region $R + \Delta R = [1, 2.50]$ Å, it was not possible to fit simultaneously all these contributions. Then, the number of C_1 and O_2 atoms and the distance Tc–C_1 and Tc–O_2 were fixed to those determined for $Tc_2(O_2CCH_3)_4Cl_2$. The results indicate presence of Tc atom at 2.19(1) Å, Br atoms at 2.63(1) Å and O atoms at 2.03(1) Å.
- The distance Tc_1–Br_1 was fixed to the value determined in the first iteration. The number of atoms was fixed to 1 for Tc_2, 4 for O_1, 1 for Br_1, 4 for O_2 and 4 for C_1. Except for Tc_1–Br_1, all the distances were allowed to vary. The results indicate the presence of O_2 atoms at 2.98(1) Å. In a similar iteration the distance Tc–C_1 was determined at 2.86(1) Å.
- In the last iteration, all the distances were allowed to vary. The σ^2 were fixed to the value determined before and the numbers of atoms fixed to 4 for O_1, O_2 and C_1 and to one for Tc_2 and Br_1.

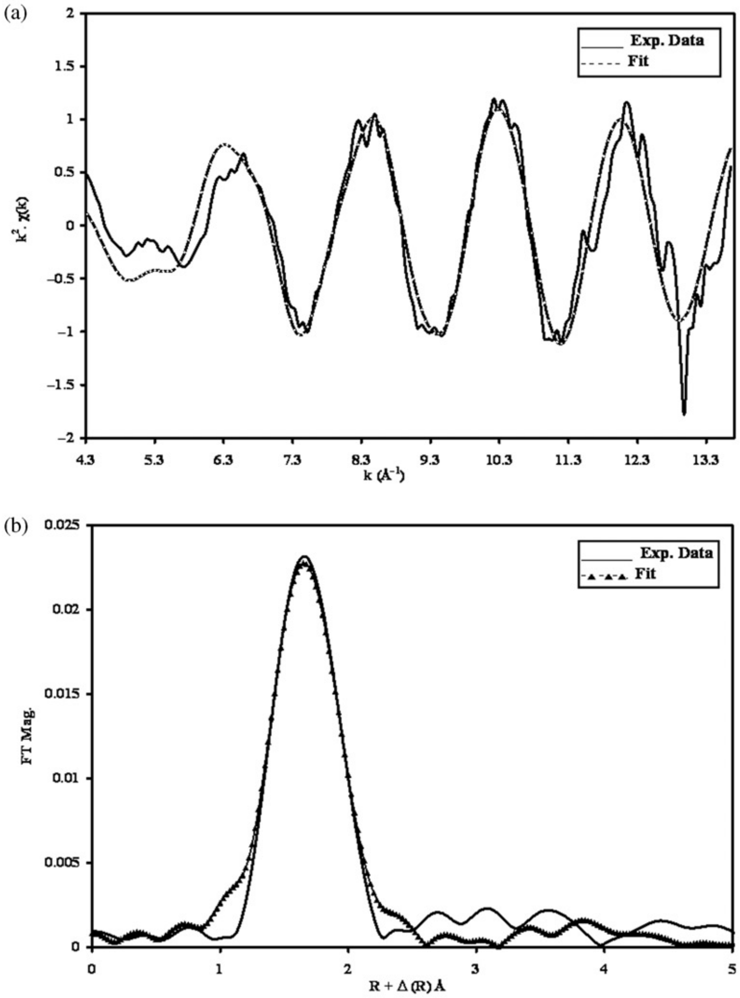

Figure 5. Fitted Experimental k^2-EXAFS spectra (a) and Fourier transform of k^2-EXAFS spectra (b) of $Tc_2(O_2CCH_3)_4Cl_2$ Adjustment between $k = [4.2, 13.7]$ Å^{-1}.

Table 2. Structural parameter obtained by adjustment of the k^2-EXAFS spectra of $Tc_2(O_2CCH_3)_4Cl_2$.

	Structural parameter		
Scattering	C.N	R (Å)	σ^2 (Å^2)
A: Tc_1–Tc_2	1	2.18	0.001
B: Tc_1–Cl_1	1	2.43	0.012
C: Tc_1–O_1	4	2.03	0.0006
D: Tc_1–C_1	4	2.86	0.0030
E: Tc–O_2	4	2.97	0.0074
F	8	3.10	0.005
G	4	4.06	0.01
H	1	4.66	0.01

Adjustment between $k = [4.2, 13.7]$ Å^{-1}. Residual = 17%. ΔE_0 (eV) = −10.17 eV.

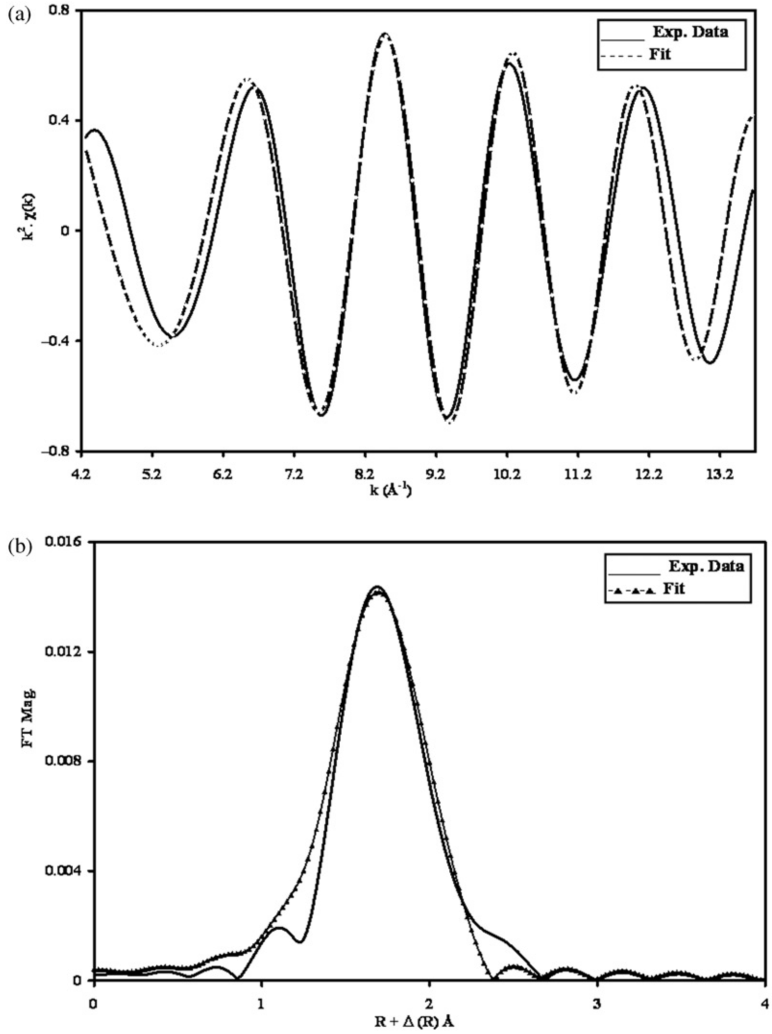

Figure 6. Adjustment of filtered Fourier transform (b) and back transformed k^2-EXAFS (a) spectra of $Tc_2(O_2CCH_3)_4Br_2$. Fourier Filtering between $R + \Delta R = [1, 2.50]$ Å; adjustment between $k = [4.2, 13.7]$ Å^{-1}.

Table 3. Structural parameter for $Tc_2(O_2CCH_3)_4Br_2$ obtained after Fourier Filtering between $R + \Delta R = [1, 2.50]$ Å.

	Structural parameter		
Scattering	C.N	R (Å)	σ^2 (Å^2)
A: Tc_1–Tc_2	1	2.19	0.0028
B: Tc_1–Br_1	1	2.63	0.0084
C: Tc_1–O_1	4	2.03	0.0055
D: Tc_1–C_1	4	2.86	0.0052
E: Tc–O_2	4	2.98	0.0088

Adjustment between $k = [4.2, 13.7]$ Å^{-1}. Residual = 11.7%. ΔE_0 (eV) = −7.84 eV.

The fitted Fourier transform and k^2-EXAFS spectra are shown in figure 6. The structural parameters are presented in table 3. Results indicate that the first coordination shell around the absorbing atom has one Tc atom at 2.19(1) Å, one Br atom at 2.63(1) Å and four O atoms at 2.03(1) Å.

b. Adjustment of the total EXAFS spectra. The total EXAFS spectrum was adjusted between [4.2, 13.7] $Å^{-1}$ using the scattering wave functions determined in **3.1** according the following procedure:

- The number of Tc_2, Br_1, O_1, C_1, and O_2 atoms and the corresponding distances were fixed to the values previously determined in **3.2.2.a**.
- The degeneracy of the multi scattering F, G, and H were fixed to the value determined in **3.1**.
- The scattering length of F, G, H and all the σ^2 were allowed to vary.

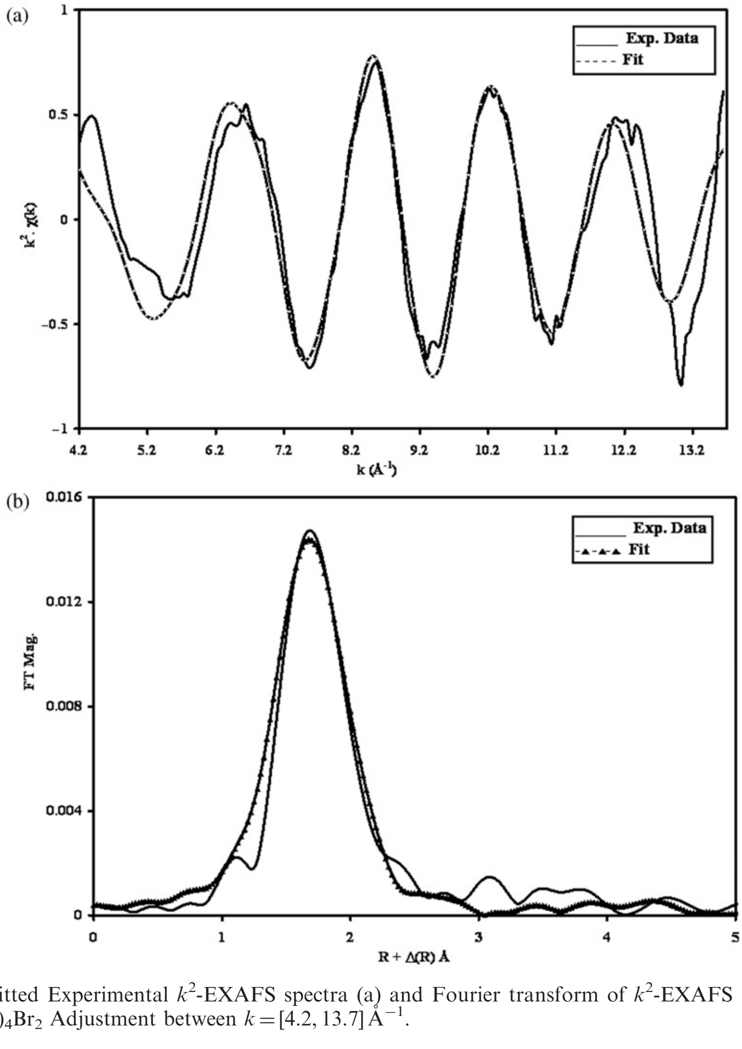

Figure 7. Fitted Experimental k^2-EXAFS spectra (a) and Fourier transform of k^2-EXAFS spectra (b) of $Tc_2(O_2CCH_3)_4Br_2$ Adjustment between $k = [4.2, 13.7]\,Å^{-1}$.

Table 4. Structural parameter obtained by adjustment of the k^2-EXAFS spectra of $Tc_2(O_2CCH_3)_4Br_2$.

	Structural parameter		
Scattering	C.N	R (Å)	σ^2 (Å^2)
A: Tc_1–Tc_2	1	2.19	0.0024
B: Tc_1–Br_1	1	2.63	0.0090
C: Tc_1–O_1	4	2.03	0.0049
D: Tc_1–C_1	4	2.86	0.0046
E: Tc–O_2	4	2.98	0.0060
F	8	3.08	0.0130
G	4	4.06	0.0170
H	1	4.84	0.0180

Adjustment between $k = [4.2, 13.7]$ Å^{-1}. Residual = 18.4%. ΔE_0 (eV) = −7.86 eV.

The fitted Fourier transform and k^2-EXAFS spectra are shown in figure 7. The structural parameters are presented in table 4.

For $Tc_2(O_2CCH_3)_4Br_2$, the first coordination shell around the absorbing atom has one Tc atom at 2.19(1) Å, one Br atom at 2.63(1) Å and four O atoms at 2.03(1) Å. The second coordination shell is constituted by four C atoms at 2.86(1) Å and the third coordination shell by four O atoms at 2.98(1) Å.

4. Discussion

The structural data determined above are compared with those derived by Raman spectroscopy [4] (table 5). The distance for Tc_1–Tc_2 and Tc–O_1 obtained by XAFS and Raman spectroscopy are in good agreement, while the Tc_1–X_1 distances determined by EXAFS are longer: ~ 0.03(1) Å for X = Cl, Br. Possibly the Tc–X distances determined by EXAFS are over-estimated. Previous studies [2, 19] on $(n\text{–}Bu_4N)_2M_2Cl_8$ (M = Tc, Re) show that the M–M distance determined by XAFS is in agreement with the crystallographic data while the M–Cl distances are longer (0.04 Å for Re–Cl and 0.02 Å for Tc–Cl). This error is due to the fact that the phase and amplitude corresponding to M–Cl and M–M scattering are close on the Fourier Transform (figure 1).

The Tc–Tc separation in $Tc_2(O_2CCH_3)_4X_2$ (X = Cl, Br) is compared with those of other quadruply bonded technetium dimers (table 5). The Tc–Tc and Tc–Cl distances, i.e, 2.18(1) Å and 2.43(1) Å, determined by EXAFS for $Tc_2(O_2CCH_3)_4Cl_2$ are similar to the ones found by XRD for $Tc_2(O_2CCMe_3)_4Cl_2$, i.e., Tc–Tc = 2.192(1) Å, Tc–Cl = 2.408(4) Å.

The carboxylate compounds exhibit longer Tc–Tc separations; the difference of the Tc–Tc separation in technetium dimers is discussed as a function of (i) the position and (ii) the nature of the terminal ligand.

(i) Position of the ligand. An elongation of 0.03(1) Å of the Tc–Tc distance is noted when moving from $(n\text{–}Bu_4N)_2Tc_2X_8$ to $Tc_2(O_2CCH_3)_4X_2$ (X = Cl, Br). The carboxylate dimers have axial halide coordination, while the octahalogeno compounds possess only equatorially coordinated halides. It was previously suggested [21] that the presence of strong axial ligands in $M_2(O_2CR)_4X_2$ should lead to lengthening of M–M bonds. This "trans-effect" phenomenon was explained considering that the only d orbital

Table 5. Interatomic distance (Å): Tc–Tc, Tc–X (X = Cl, Br), Tc–O_{ax} and Tc–O_{eq} in technetium quadruply bonded dimers.

Compounds	*d* TcTc	*d* TcX_{term}	*d* TcO_{eq}	*d* TcO_{ax}	Reference
$(n\text{–Bu}_4\text{N})_2\text{Tc}_2\text{Cl}_8$	2.147(4)	2.320(4)-eq	–	–	[24]
$(n\text{–Bu}_4\text{N})_2\text{Tc}_2\text{Br}_8$	2.15(1)	2.48(1)-eq	–	–	[2]
$\text{Tc}_2(\text{O}_2\text{CCH}_3)_4\text{Cl}_2$	2.18(1)	2.43(1)-ax	2.03(1)	–	This work
	2.192	**2.408**	**2.032**		[4]
$\text{Tc}_2(\text{O}_2\text{CCH}_3)_4\text{Br}_2$	2.19(1)	2.63(1)-ax	2.03(1)		This work
	2.192	**2.600**	**2.032**		[4]
$\text{Tc}_2(\text{O}_2\text{CCMe}_3)_4\text{Cl}_2$	2.192(1)	2.408(4)-ax	2.032(4)	–	[6]
$\text{K}_2\text{Tc}_2(\text{SO}_4)_4.2\text{H}_2\text{O}$	2.155(1)		2.02(1)	2.249	[21]
$\text{Tc}_2(\text{O}_2\text{CCH}_3)_4(\text{TcO}_4)_2$	2.149(1)	–	2.014(15)	2.153(5)	[20]

Values in bold were determined by Raman spectroscopy.

Table 6. Interatomic distance (Å): Re–Re, Re–X (X = Cl, Br), Re–O_{ax} and Re–O_{eq} in rhenium quadruply bonded dimers.

Compounds	*d* ReRe	*d* ReX_{term}	*d* ReO_{eq}	*d* ReO_{ax}	Reference
$(n\text{–Bu}_4\text{N})_2\text{Re}_2\text{Cl}_8$	2.222(1)	2.32(1)-eq	–	–	[25]
$(n\text{–Bu}_4\text{N})_2\text{Re}_2\text{Br}_8$	2.218	2.473-eq	–	–	[26]
$\text{Re}_2(\text{O}_2\text{CCH}_3)_4\text{Cl}_2$	**2.224**	**2.521-ax**	**2.022**		[4]
	2.224	2.521	2.018		[28]
$\text{Re}_2(\text{O}_2\text{CCH}_3)_4\text{Br}_2$	**2.224**	**2.603-ax**	**2.022**		[4]
$\text{Re}_2(\text{O}_2\text{CCMe}_3)_4\text{Cl}_2$	2.236(1)	2.477(3)-ax	2.025(4)	–	[15]
$\text{Re}_2(\text{O}_2\text{CCMe}_3)_4\text{Br}_2$	2.234(1)	2.603(1)-ax	2.029(5)		[15]
$\text{K}_2\text{Re}_2(\text{SO}_4)_4.2\text{H}_2\text{O}$	2.214(1)			2.28	[27]

Values in bold were determined by Raman spectroscopy.

available for σ bonding is shared between M–M and M–X bonds. A competitive situation is created and stronger M–X σ-bonding will lead to weaker M–M σ-bonding. Since M–M σ bonding is an important component of the quadruple bond, strong M–X bonding should lengthen the M–M bond.

Structural analysis of analogous Re compounds (table 6) indicate that the position of ligand has a minimal impact on Re–Re separation; an elongation of 0.002(1) Å is noted when moving from $(n\text{–Bu}_4\text{N})_2\text{Re}_2\text{X}_8$ to $\text{Re}_2(\text{O}_2\text{CCH}_3)_4\text{X}_2$ (X = Cl, Br). The "trans-effect" is obviously stronger for technetium than for rhenium quadruply bonded dimers.

(ii) Nature of the axial ligand. A diminution of 0.03(1) Å of the Tc–Tc separation is noted when moving from $\text{Tc}_2(\text{O}_2\text{CCH}_3)_4\text{X}_2$ (X = Cl, Br) to $\text{Tc}_2(\text{O}_2\text{CCH}_3)_4(\text{TcO}_4)_2$ [20, 21], i.e., replacing a pertechnetate by a chloride leads to lengthening of the Tc–Tc bond. This suggests that the Tc–Cl bond is more covalent than the Tc–OTcO_3 bond which seems eminently reasonable.

5. Conclusion

EXAFS measurements on Tc carboxylate compounds have permitted us to determine interatomic distances for the first (Tc–Tc, Tc–O, Tc–X), second (Tc–C) and third coordination shells (Tc–O) around the Tc atom. The Tc–Tc separation in $Tc_2(O_2CCH_3)_4X_2$ (X=Cl, Br) is the largest noted among all the quadruply bonded Tc dimers whose structures have been determined thus far. This phenomenon is due to the presence of strong axial ligands which weaken the Tc–Tc σ-bond and increase the Tc–Tc separation. The nature of the axial ligand also has an influence on the Tc–Tc separation. A longer Tc–Tc separation in $Tc_2(O_2CCH_3)_4X_2$ (X = Cl, Br) than in $Tc_2(O_2CCH_3)_4(TcO_4)_2$ indicates that axial chloride and bromide ligands are better σ-donors and exert a greater trans influence on the Tc–Tc quadruple bond than the axial pertechnetate ligand. In the analogous Re compounds the axial halide ligand has a very minor influence on Re–Re separation. In order to better understand the influence of axial and equatorial ligands on Tc–Tc separations in quadruply bonded dimers, it will be necessary to increase the number and variety of such complexes. Work along these lines is in progress.

Acknowledgments

Use of the Advanced Photon Source was supported by the U. S. Department of Energy, Office of Science, Office of Basic Energy Sciences, under Contract No. DE-AC02-06CH11357. We are grateful to Dr. Carol J. Burns, Los Alamos National Laboratory, for a generous loan of ammonium pertechnetate. The authors thank Mr. Tom O'Dou (UNLV) for exceptional health physics support.

References

[1] A.P. Sattelberger. In *Multiple Bonds between Metal Atoms*, 3rd Edn, F.A. Cotton, C.A. Murillo, R.A. Walton (Eds), Springer, New-York (2005).
[2] F. Poineau, A.P. Sattelberger, S.D. Conradson, K.R. Czerwinski. *Inorg. Chem.*, in press.
[3] L.L. Zaitseva, A.S. Kotel'nikova, A.A. Rezvov. *Zh. Neorg. Khim.*, **25**, 2624 (1980).
[4] J. Skowronek, W. Preetz. *Z. Naturforsch.*, **47B**, 482 (1992).
[5] C.M. Kennedy, T.C. *Int. J. Radiat. Appl. Instrum. Part A. Appl. Radiat. Isot.*, **11**, 1167 (1988).
[6] F.A. Cotton, L.D. Gage. *Nouv. J. Chim.*, **1**, 441 (1977).
[7] I. Almahamid, J.C. Bryan, J.J. Bucher, A.K. Burrell, N.M. Edelstein, E.A. Hudson, N. Kaltsoyannis, W.W. Lukens, D.K. Shuh, H. Nitsche, T. Reich. *Inorg. Chem.*, **34**, 193 (1995).
[8] R.W. Thomas, M.J. Heeg, R.C. Elder, R. Deutsch. *Inorg. Chem.*, **24**, 1472 (1985).
[9] W.W. Lukens, J.J. Bucher, N.M. Edelstein, D.K. Shuh. *Environ. Sci. Technol.*, **36**, 1124 (2002).
[10] W. Preetz, G. Peters, D. Bublitz. *J. Clust. Sci.*, **5**, 83 (1994).
[11] M. Newville, P. Livins, Y. Yacoby, E.A. Stern, J.J. Rehr. *Phys. Rev.*, **B47**, 14126 (1993).
[12] T. Ressler. *J. Synchrotron Rad.*, **5**, 118 (1998).
[13] J.J. Rehr, R.C. Albers. *Rev. Mod. Phys.*, **72**, 621 (2000).
[14] B. Ravel. *J. Synchrotron Rad.*, **8**, 314 (2001).
[15] D.M. Collins, F.A. Cotton, L.D. Gage. *Inorg. Chem.*, **18**, 1712 (1979).
[16] A. Maes, K. Geraedts, C. Bruggeman, J. Vancluysen, A. Rossberg, C. Hennig. *Environ. Sci. Technol.*, **38**, 2044 (2004).
[17] B. Ravel, M. Newville. *J. Synchrotron Rad.*, **12**, 537 (2005).
[18] B. K Teo. *J. Am. Chem. Soc.*, **103**, 3990 (1981).
[19] S.D. Conradson, A.P. Sattelberger, W.H. Woodruff. *J. Am. Chem. Soc.*, **110**, 1309 (1988).
[20] N.A. Baturin, K.E. German, M.S. Grigor'ev, S.V. Kryuchkov. *Koordinats. Khim.*, **17**, 1375 (1991).
[21] S.V. Kryutchkov. *Top. Curr. Chem.*, **176**, 189 (1996).
[22] W. Preetz, L. Rudzik. *Angew. Chem.*, **91**, 159 (1979).
[23] G. Peters, W. Preetz. *Z. Naturforsch.*, **34B**, 1767 (1979).
[24] F.A. Cotton, L. Daniels, A. Davison, C. Orvig. *Inorg. Chem.*, **20**, 3051 (1981).

[25] F.A. Cotton, B.A. Frenz, B.R. Stults, R. Webb. *J. Am. Chem. Soc.*, **98**, 2768 (1976).
[26] H.W. Huang, D.S. Martin. *Inorg. Chem.*, **24**, 96 (1985).
[27] P.A. Koz'min, T.B. Larina, M.D. Surazhskaya, A.S. Kotel'nikova, N.S. Osmanov. *Koordinats. Khim.*, **6**, 1264 (1980).
[28] P.A. Koz'min, M.D. Surazhskaya, T.B. Larina, A.S. Kotel'nikova, T.V. Misailova. *Koordinats. Khim.*, **6**, 1256 (1980).